JOURNAL OF GEOPHYSICAL RESEARCH, 94, NO. B12, PAGES 17,729–17,733, DECEMBER 10, 1989

Nonlinear Generation of Elastic Waves in Granite and Sandstone: Continuous Wave and Travel Time Observations

PAUL A. JOHNSON AND THOMAS J. SHANKLAND

Los Alamos National Laboratory, Los Alamos, New Mexico

Beams generated by nonlinear interaction have proved useful as low-frequency, highly directional sources in water and may ultimately find application in geophysical exploration. For nonlinear elastic waves to be used as seismic sources they must be detected as discrete arrivals; measuring travel times of pulsed, nonlinear beams is a necessary first step toward that end. In this paper we discuss two new observations of the interaction of nonlinear elastic waves in both crystalline rock and sandstone. We show that observed travel times of pulsed waves agreed with predicted times for the case where two P wave pulses interacted to produce an S wave pulse. The travel time measurement was difficult to obtain because conversion efficiency is low. In extending our continuous wave experiments to sandstone we also satisfied three criteria previously verified in crystalline quartz norite and in granite to demonstrate nonlinear interaction: (1) the frequency of the nonlinear-generated signal equalled the difference frequency $f_1 - f_2$ when two P waves interacted to produce an S wave, (2) the amplitude of the signal was proportional to the amplitude product of the primary waves, and (3) in the case of intersecting P waves the trajectory of the nonlinear beam matched that predicted by nonlinear elasticity theory.

INTRODUCTION

Properties of nonlinear elastic materials have been rigorously studied in the field of acoustics over the last three decades. *Westervelt* [1963] was the first to show that two near-source, collinear (parallel), high-frequency primary waves could interact to produce acoustic waves with frequencies equal to the sum and difference frequencies of the primaries. Further, these waves showed directional radiation patterns (beams), as predicted by nonlinear elasticity theory. The generation of the sum and difference frequency beams is inefficient; nonetheless, the difference frequency beam proved to be useful as a directional, low-frequency source because of its radiation pattern. Many experiments leading to practical applications followed Westervelt's, including those by *Bellin and Beyer* [1962] and *Muir and Willette* [1972]. To date, nonlinear beam generation has led to developments in echo sounding, underwater communications, and shallow sediment probing beneath water [*Nichols*, 1971].

In geophysics, elastic nonlinearity has been modeled using equations of state containing nonlinear contributions appearing as third-order or higher terms in the elastic free energy expansion. In materials such as water, metals, or single crystals where numerous measurements of nonlinear elasticity have been obtained [e.g., *Anderson and Suzuki*, 1983; *Hiki and Mukai*, 1973; *Rollins et al.*, 1964], the higher-order contributions are small, resulting entirely from lattice anharmonicity. When two high-frequency beams are mixed in intact (uncracked) material, the weak higher-order contributions result in relatively low-amplitude difference frequency beams. However, materials such as rock are inherently more nonlinear than other materials because their microcracks give rise to large changes of velocity (or moduli) with pressure [*Birch*, 1960]; thus rocks have larger higher-order terms. When two high-frequency beams are mixed in rock, a large-amplitude difference frequency beam is produced because the amplitude of the nonlinear-generated wave is proportional to the value of the higher-order terms [e.g., *O'Connell and Budiansky*, 1977; *Winkler et al.*, 1979; *Carlson and Gangi*, 1985]. The dimensionless parameter to describe a change of an elastic modulus C with pressure P is $M = dC/dP = (2\rho v\, dv/dP)$, where ρ is density and v is a velocity. In most materials, M is 4–6; for instance, this is the approximate variation dK/dP of bulk modulus K. For rocks, however, M can be 2 orders of magnitude greater.

Conservation of energy and momentum requires that certain relationships exist between frequency, velocity, and interaction angles when two noncollinear beams of different frequencies are mixed in a rock. For the case where two P waves interact to produce a scattered S wave the relations are

$$\cos\phi = \frac{1}{c^2} - \frac{(1-c^2)(a^2+1)}{2ac^2} \tag{1}$$

$$\tan\gamma = \frac{-a\sin\phi}{1-a\cos\phi} \tag{2}$$

where ϕ is the angle between k_1 and k_2 shown in Figure 1, γ is the angle between k_1 and k_3 in Figure 1, c is the velocity ratio v_s/v_p, and a is the frequency ratio f_2/f_1. The scattered S wave is polarized in the plane formed by $k_1 - k_2 - k_3$ [*Jones and Kobett*, 1963; *Taylor and Rollins*, 1964]. It is clear from (1) and (2) that once either input angle, output angle, or frequency is selected for a given velocity ratio, the two remaining parameters are fixed.

In a previous paper [*Johnson et al.*, 1987], we reported observations of nonlinear, high-frequency elastic wave interaction in two crystalline rocks: Berkeley blue granite (Elberton, Georgia) and Starlight black quartz norite (Belfast, South Africa). We observed elastic nonlinearity when two waves of frequencies f_1 and f_2 interacted in these rocks to produce a wave at the difference frequency $f_1 - f_2$. This observation confirmed the existence of a nonlinear interaction that obeyed the selection rules derived from the nonlin-

Paper number 89JB01536.
0148-0227/89/89JB-01536$05.00

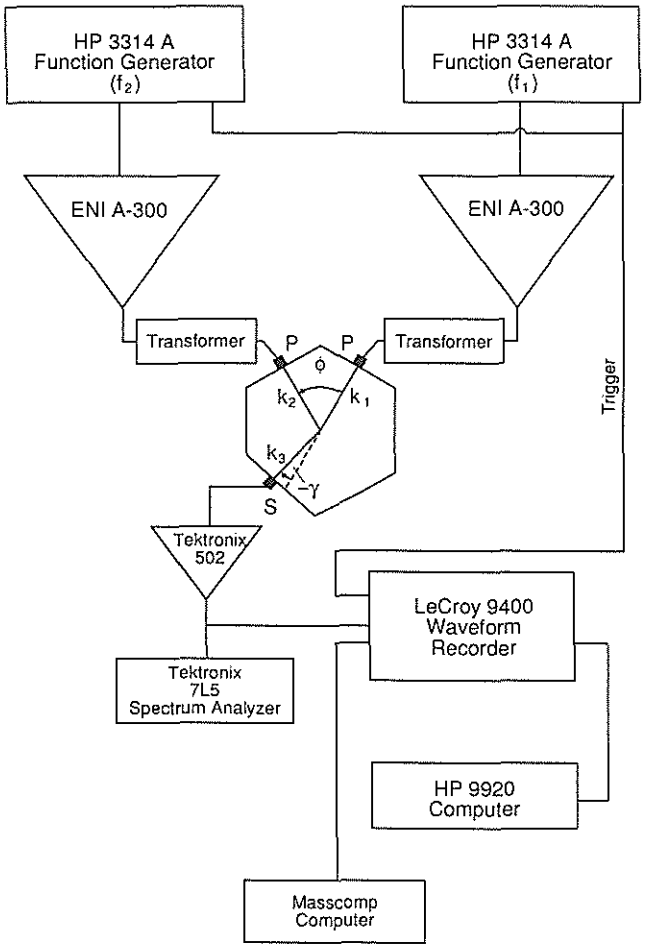

Fig. 1. Block diagram of experimental configuration. The k_1, k_2, and k_3 refer to wave propagation directions, and ϕ and γ show interaction geometry angular relationships. P and S are P wave and S wave transducers, respectively.

ear wave equation. In our latest experiments, (1) we demonstrate that nonlinear interaction takes place in sandstone in the same manner as that described by *Johnson et al.* [1987] for crystalline rock, and (2) we further characterize nonlinear interaction in both kinds of rock: when two noncollinear pulsed P waves intersect to produce an S wave pulse, the observed travel time of the nonlinear-generated signal matches the predicted value. This is the first verifiable travel time observation of a nonlinear-generated signal in rock. We use the terms "difference frequency signal" and "nonlinear-generated signal" synonymously throughout the following discussion.

BEAM MIXING MEASUREMENTS

Our earlier experiments focused on two beam-mixing geometries: collinear and noncollinear of which the noncollinear case is more general. For the case of noncollinear mixing, we conducted two categories of experiments: one in which two P waves interacted to produce an S wave, and another in which P and S waves interacted to produce a P wave.

In previous experiments we used three criteria derived from the selection rules to verify that nonlinear mixing took place in rock: (1) the frequency of the nonlinear-generated signal had to be precisely equal to the difference frequency $f_1 - f_2$; (2) the amplitude of the difference frequency had to be proportional to the product of the amplitudes of the primary beams, and (3) the trajectory and frequency ratios of the nonlinear-generated signal had to match those predicted by the selection rules. In this paper we report results from granite and sandstone samples based on these same criteria. Further, pulsed beams satisfied the additional criterion that the predicted travel time of the nonlinear-generated signal matched the observed travel time. The noncollinear case of two P waves interacting to produce an S wave was also used in these experiments.

TABLE 1. Measured Rock Velocities

	v_p, km/s	v_s, km/s
Berkeley blue granite	3.33	2.26
Berea sandstone	2.78	1.77

We chose Berkeley blue granite (Elberton, Georgia) and Berea sandstone (Ohio) (hereafter referred to as granite and sandstone) since their physical characteristics are well known [e.g., *Krech et al.*, 1974; *Halleck and Cumnick*, 1980]. Table 1 shows the average velocities for the samples that we used. We obtained the velocity measurements by taking the average P and S wave velocities in three perpendicular directions in both samples. These velocities were used in calculating the angles, ϕ and γ. Figure 1 shows the experimental configuration slightly modified from that described by *Johnson et al.* [1987]. In these experiments the function generators provided either continuous monochromatic sine waves or pulses. These signals were amplified by separate power amplifiers and directed into the rock via piezoelectric transducers (PZTs) bonded to the rock with phenyl salicylate. Typical signal path lengths were about 17 cm, typical wavelengths were 1 cm, and grain sizes were less than 1.0 mm in the sandstone and 0.5–2.0 mm in the granite. The transmitted signal was detected by a third PZT, amplified, and observed on a spectrum analyzer or a waveform recorder. The PZTs are 1 inch in diameter and are manufactured by Panametrics, Incorporated; the two primaries have center frequency responses of 0.5 MHz, and the S wave detector has a center frequency response of 0.25 MHz. Notable experimental improvements from the earlier experiments were the addition of transformers for electrical impedance matching between the power amplifiers and transducers, the addition of a digital oscilloscope (LeCroy 9400), and the use of signal processing software on a MASSCOMP computer. The oscilloscope allowed us to capture, average, and analyze discrete pulses and continuous wave (CW) signals and to carry out processing such as fast Fourier transforms (FFTs). Signals were plotted directly from the oscilloscope or were transferred for storage and further processing on a Hewlett-Packard 9920 or MASSCOMP computer.

Amplitude Measurements

We conducted amplitude measurements in both CW and pulsed mode to test criterion 1 (the difference frequency equals $f_1 - f_2$) and criterion 2 (the amplitude product of the primary beams is proportional to the difference frequency

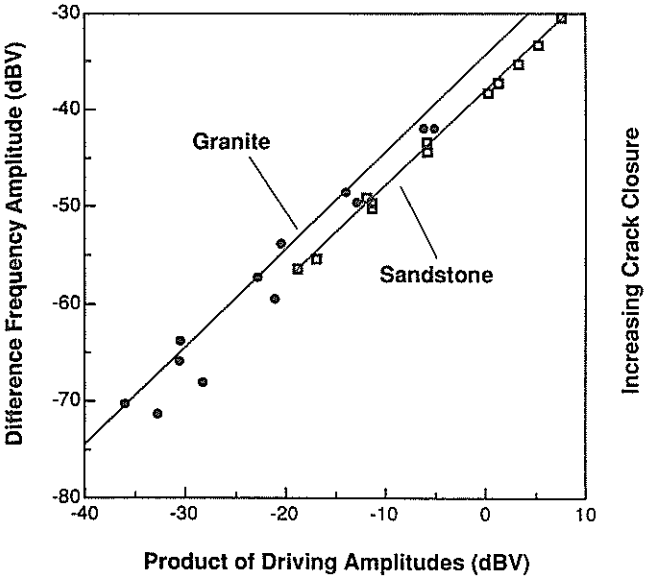

Fig. 2. Proportionality of the amplitude dependence of the difference frequency to the product of the primary beam amplitudes. Qualitative increase in crack closure with increasing product of primary beam amplitudes is shown on right-hand ordinate. Accuracy of measurement is better than ±2 dB V (dB V refers to decibel referenced to 1 volt).

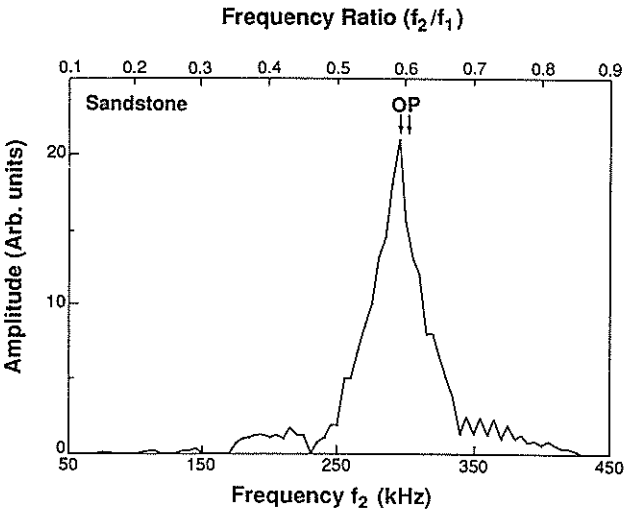

Fig. 3. Amplitude dependence of the difference frequency beam to f_2 for the sandstone. The predicted peak amplitude should occur at $f_2/f_1 = 0.61$, or $f_2 = 305$ kHz (P). The actual peak occurs at $f_2/f_1 = 0.59$, or 295 kHz (O).

beam amplitude). In these experiments we recorded the primary beam and difference frequency beam amplitudes while increasing input amplitudes. Figure 2 shows that criterion 2 was indeed satisfied for the granite and sandstone. Also indicated in Figure 2 is a qualitative relationship between crack closure and the product of the driving beam amplitudes. (Criterion 1 was also satisfied merely by observation of the difference frequency signal.)

Frequency Sweep Tests

Nonlinear mixing of the two primary frequencies within the electronic equipment can produce a difference frequency signal (intermodulation distortion) if the instruments are of poor quality or are not properly isolated; surface wave interaction between primary transducers might also produce the signal. Criteria 1 and 2 cannot be used to distinguish between a difference frequency beam generated in the rock and a spurious signal. We therefore used angular discrimination (criterion 3) to prove that the nonlinear-generated signal was generated in the rock. That is, once the angle between input transducers is determined, the frequency ratio and output angle are fixed. If the frequency ratio is incorrect for a set geometry of input transducers, no difference frequency signal is generated. Because a nonlinear signal generated outside the rock by intermodulation distortion or surface wave interaction exists independently, response of amplitude as a function of frequency is a stringent test.

As in the work of *Johnson et al.* [1987], we arbitrarily chose the angle between input transducers so that the frequency ratio and output angle were set by criterion 3. One input frequency was held fixed, while the other input frequency was swept over an interval containing the correct frequency to produce the difference frequency beam inside the rock. Observing a maximum amplitude of the nonlinear-generated signal at the correct frequency ratio rather than over the entire sweep interval proved that the mixing took place in the rock.

An angle of 34° between input transducers for the sandstone required the output angle and frequency ratio f_2/f_1 to be −34.5° and 0.61, respectively. We held f_1 at 500 kHz and constant CW driving voltage, while sweeping f_2 from 45 to 455 kHz and recording the difference frequency signal amplitude of 5-kHz intervals of f_2. Criterion 3 predicted a maximum amplitude response when f_2 was 305 kHz (a frequency ratio f_2/f_1 of 0.61) for a nonlinear-generated signal produced by mixing inside the rock. When we varied f_2 away from 305 kHz, the nonlinear-generated signal amplitude should have vanished.

As shown in Figure 3, the maximum amplitude appeared at a difference frequency of 295 kHz (frequency ratio of 0.59), very close to the predicted value. The width of the amplitude curve is probably due to velocity anisotropy in the sandstone (about 7% for *P* waves and 6% for *S* waves) and to the large interaction volume. The relatively large interaction volume may have the effect of smearing the correct frequency ratio over a range of values centered about the predicted value. (The nonlinear elastic wave equation from which the selection rules were derived assumes a homogeneous, isotropic medium.) Sweep tests conducted in the granite produced a similar, slightly broader peak.

Travel Time Measurements

The predicted and observed difference frequency travel times in both the granite and sandstone matched closely. The predicted arrival time is calculated from the average rock velocity and distances for *P* waves propagating from the sources to the mixing region, plus *S* waves traveling from the mixing region to the detector. Travel times have been difficult to measure for several reasons: the amplitude conversion efficiency between the primary beams and difference frequency beam is generally less than 1% [*Taylor and Rollins*, 1964], elastic wave attenuation decreases the difference frequency beam amplitude, and the difference fre-

quency signal arrives after the direct P waves and is thus masked by their coda.

We therefore used the following technique to remove the primary beams from the total received signal passing through the rock, so that a nonlinear-generated signal travel time could be measured. (1) To improve signal/noise, 500 pulsed signals containing f_1, f_2, and the difference-frequency signal were summed, averaged, and stored in the LeCroy 9400. (2) The f_2 source was then turned off. The f_1 signal was summed and averaged in the same manner and then subtracted from the signal containing f_1, f_2, and the difference frequency signal. The resultant signal containing only f_2 and the difference-frequency signal was stored. (3) The f_1 source was then turned off, the f_2 source was turned on, and the f_2 signal was summed, averaged, and subtracted from the stored signal, theoretically leaving only the difference frequency signal. Expressed mathematically, the summation averaging and subtraction is

$$\left[\sum_{1}^{n}(A_{f_1}+A_{f_2}+A_{\Delta f})/n - \left(\sum_{1}^{n}A_{f_1}\right)\Big/n - \left(\sum_{1}^{n}A_{f_2}\right)\Big/n\right] \quad (3)$$

where A_{f_1} and A_{f_2} are amplitudes of the primary frequencies, $A_{\Delta f}$ is the difference frequency amplitude, and n is 500.

The subtraction is not perfect, however, and in general, small amounts of both primary signals appear in the subtracted signal. Imperfect subtraction results from the following three reasons. First, the quality of the phenyl salicylate bond varies slightly with variations in temperature and humidity, and thus amplitudes are slightly variable. Second, when the primary beams are operated independently, their received signal amplitudes are slightly larger than those in the mixed signal from which some energy has been transformed into creating the difference frequency signal. A third cause results from a small amount of trigger jitter (one of the function generators is used as a trigger source); this problem was significantly reduced by using a high sampling rate (50×10^6 samples/s).

Figures 4*a* and 4*b* show the travel time results for the granite and sandstone, respectively. The top trace in each case is the summed, unsubtracted ($A_{f_1} + A_{f_2} + A_{\Delta f}$) signal and the bottom trace is the subtracted result. To eliminate more of the remaining primary beams, the subtracted signals were passed through two-pole, low-pass digital Bessel filters with cutoff frequencies of 200 kHz.

Arrows mark the arrival times of f_1, f_2, and the nonlinear-generated signal predicted (P), and observed (O) times. The observed f_1 and f_2 arrivals were measured with each beam operating separately, whereas the nonlinear signal arrivals were determined by using changes in frequency and amplitude. The predicted arrival time of the nonlinear-generated signal in the granite is approximately 69.2 μs, while the observed value is 67 μs (arrow just left of predicted arrival). We chose this onset time based on the clear change in amplitude; however, we cannot discount the other two earlier arrivals (also marked with arrows) as being the onset of the nonlinear-generated signal. For the sandstone the predicted travel time of the nonlinear-generated signal was 75.8 μs, and the observed value was 73 μs. The onset of the nonlinear-generated signal is unmistakable in the sandstone. We attribute the difference between observed and predicted travel times to velocity anisotropy.

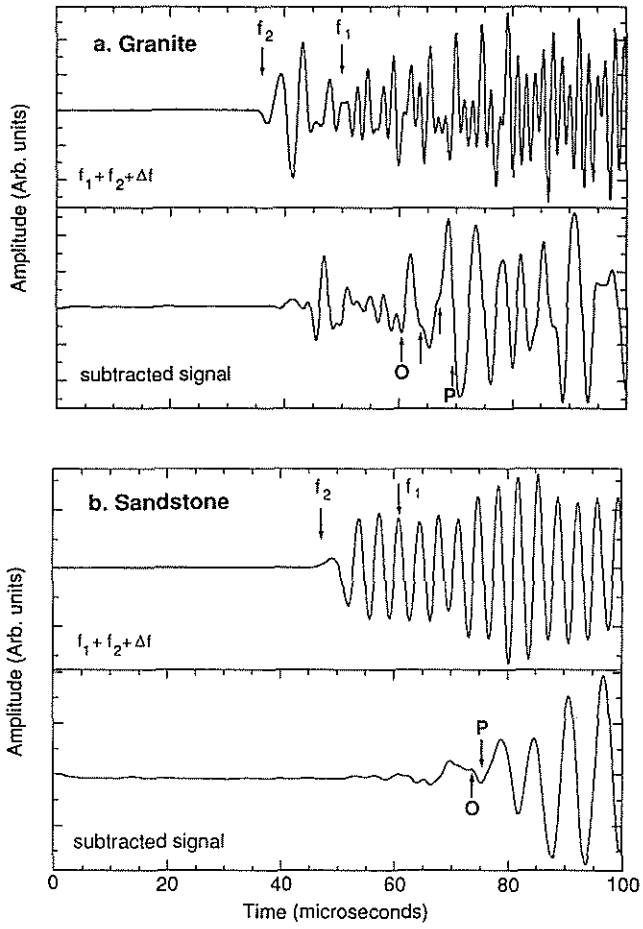

Fig. 4. Time traces comparing the original signal containing f_1, f_2 (top trace in both Figures 4*a* and 4*b*) and the difference frequency signal (bottom trace in each figure) for granite and sandstone. For the granite, f_1, f_2, and the difference frequency are 641, 466, and 175 kHz, respectively. For the sandstone, f_1, f_2, and the difference frequency are 450, 288, and 162 kHz, respectively. Predicted arrival times of f_2 and f_1 are shown by arrows in unsubtracted signals. The granite has three possible onsets for the arrival of the difference frequency (arrows). There is a vertical scale expansion of approximately 1000 times between the top and bottom traces in each case.

The spectral content of the traces in Figure 4 is shown in Figure 5. With a sampling interval of 20×10^{-9} s and 25,000 points in the FFTs the minimum frequency resolution was 2 kHz. The spectra are unsmoothed. For the combined signals the nonlinear-generated beam is lost within the noise. However, the subtracted spectra clearly show the dominant frequency to be that of the nonlinear-generated beam.

CONCLUSIONS

We demonstrated that nonlinear interaction of two high-frequency waves produces a collimated wave at their difference frequency in both granite and sandstone. We first repeated continuous wave (CW) experiments with sandstone that we had originally conducted in quartz norite. These experiments fulfill three criteria that obey selection rules derived from the nonlinear elastic wave equation. We then demonstrated a fourth criterion, that the theoretically pre-

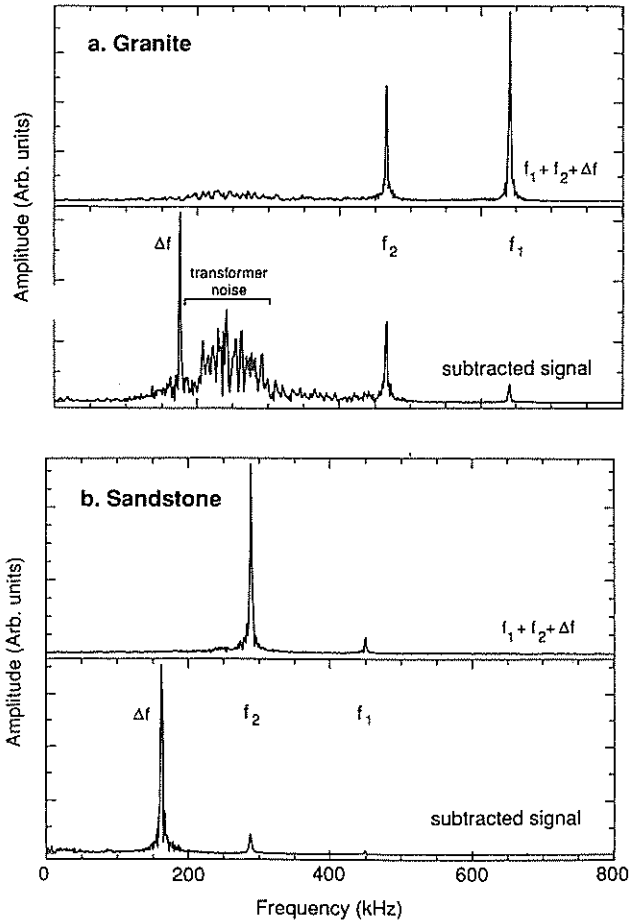

Fig. 5. Power spectral plots for the granite and sandstone before and after subtraction of f_1 and f_2. The top trace in each figure is the unsubtracted signal and bottom trace is the subtracted signal. Peaks from left to right in Figure 5*a* are at 175, 466, and 641 kHz. In Figure 5*b*, peaks are at 162, 288, and 450 kHz. The coherent noise in the subtracted-signal spectrum is from amplitude clipping inside one of the transformers; the noise disappears when this transformer is removed. There is a vertical scale expansion of approximately 1000 times between the top and bottom traces in each case.

dicted travel times of the difference frequency beams match observed travel times in crystalline rock and sandstone. This most recent characterization of the nonlinear-generated signal is important if an exploration tool is to be developed, since a pulsed beam would likely be necessary to measure direct or reflected travel times.

Acknowledgments. This work was supported by the Office of Basic Energy Sciences of the Department of Energy, under contract W-7405-ENG-36 with Los Alamos National Laboratory. We are grateful for suggestions from R. J. O'Connell, J. N. Albright, and Scott Phillips.

REFERENCES

Anderson, O. L., and I. Suzuki, Anharmonicity of three minerals at high temperature: Forsterite, fayalite, and periclase, *J. Geophys. Res.*, *88*, 3549–3556, 1983.

Bellin, J. L. S., and R. T. Beyer, Experimental investigation of an end-fire array, *J. Acoust. Soc. Am.*, *34*, 1051–1059, 1962.

Birch, F., The velocity of compressional waves in rocks to 10 kilobars, part 1, *J. Geophys. Res.*, *65*, 1083–1102, 1960.

Carlson, R. L., and A. F. Gangi, Effect of cracks on the pressure dependence of *P* wave velocities in crystalline rock, *J. Geophys. Res.*, *90*, 8675–8684, 1985.

Halleck, P. M., and A. J. Cumnick, The influence of orientation on fracture toughness and tensile moduli in Berkeley Granite, *Proc. Symp. Rock Mech.*, *21st*, 235–242, 1980.

Hiki, Y., and K. Mukai, Ultrasonic three-phonon process in copper crystal, *J. Phys. Soc. Jpn.*, *34*, 454–461, 1973.

Johnson, P. A., T. J. Shankland, R. J. O'Connell, and J. N. Albright, Nonlinear generation of elastic waves in crystalline rock, *J. Geophys. Res.*, *92*, 3597–3602, 1987.

Jones, G. L., and D. Kobett, Interaction of elastic waves in an isotropic solid, *J. Acoust. Soc. Am.*, *35*, 5–10, 1963.

Krech, W. W., F. A. Henderson, and K. E. Hjelmstad, A standard rock suite for rapid excavation research, *Rep. Invest. U.S. Bur. Mines, RI 7865*, 1974.

Muir, T. G., and J. G. Willette, Parametric acoustic transmitting arrays, *J. Acoust. Soc. Am.*, *52*, 1481–1486, 1972.

Nichols, R. H., Jr., Finite amplitude effects used to improve echo-sounder, *J. Acoust. Soc. Am.*, *50*, 1086–1087, 1971.

O'Connell, R. J., and B. Budiansky, Viscoelastic properties of fluid-saturated cracked solids, *J. Geophys. Res.*, *82*, 5719–5735, 1977.

Rollins, F. R., Jr., L. H. Taylor, and P. H. Todd, Jr., Ultrasonic study of three-phonon interactions, II, Experimental results, *Phys. Rev. Sect. A*, *136*, 597–601, 1964.

Taylor, L. H., and F. R. Rollins, Jr., Ultrasonic study of three-phonon interactions, I, Theory, *Phys. Rev. Sect. A*, *136*, 591–596, 1964.

Westervelt, P. J., Parametric acoustic array, *J. Acoust. Soc. Am.*, *26*, 535–537, 1963.

Winkler, K. W., A. Nur, and M. Gladwin, Friction and seismic attenuation in rocks, *Nature*, *277*, 528–531, 1979.

P. A. Johnson and T. J. Shankland, Los Alamos National Laboratory, D443, Los Alamos, NM 87545.

(Received December 15, 1988;
revised April 10, 1989;
accepted July 10, 1989.)